Western Region Technical Attachment
No. 95-15
May 16, 1995

OPERATIONAL USE OF POTENTIAL VORTICITY TO IDENTIFY THE LOCATION, STRENGTH AND MOVEMENT OF UPPER-LEVEL FRONTS

Chris Gibson - NWSFO Boise, ID

Introduction

The importance of upper-level frontal zones in determining middle and lower tropospheric circulation patterns, including the influence of upper-fronts on surface cyclones, is well established (Bluestein 1986; Keyser 1986; Hirschberg and Fritsch 1991). Analysis of potential vorticity (PV) identifies the location and strength of upper-level fronts, dividing tropospheric air from stratospheric air, at the level of maximum wind. The PV distribution, within the gridded model forecast data, indicates the location and relative strength of synoptic-scale weather features in the upper troposphere. For instance, PV analysis provides an excellent tool for diagnosing the location and forecast movement of weak upper-level troughs moving around, or through the western United States upper-level ridge. These systems frequently produce outbreaks of persistent nocturnal thunderstorms.

Motivation

Potential vorticity has long been recognized as an important conservative tracer of air parcels. Hoskins et al. (1985) present a complete review of early theoretical work describing PV and the potential applications of PV in operational weather analysis and forecasting. Holton (1992) presents a form of PV (Eqn. 1) known as Ertel's Potential Vorticity.

$$P \equiv (\zeta_\theta + f)\left(-g\frac{\partial \theta}{\partial p}\right) = constant \qquad (1)$$

Ertel's PV is a product of the absolute vorticity, the dry static stability and the gravitational constant (g). PV, as defined here, is conservative on an isentropic surface in a frictionless, adiabatic environment, such as in the upper troposphere and lower stratosphere.

A cross-section (Fig. 1a), through an intense upper-level low, has been constructed using the PC-GRIDDS (Meier 1993) software, with forecast data from the NGM. The cross-section includes an area of high static stability (θ increasing rapidly with height) aloft, where stratospheric air has descended into the upper troposphere, forming a tropopause "undulation". A positive cyclonic circulation is indicated by the isotachs, surrounding the undulation and extending into the lower troposphere. Lower static stability, relative to surrounding areas, indicates cold and humid air directly under the undulation, between 500 mb and the surface. Within the 200-400 mb layer, the PV is at a maximum in the center of the diagram, due to the area of high static stability and positive cyclonic vorticity located

there (Eqn. 1). In a plan view of PV calculated within this layer (Fig. 1b), a PV maximum correlates with the location of the low and tropopause undulation. The area of large PV gradient around the low diagnoses the area of sloped tropopause, and thus the upper-level frontal zone between the troposphere and stratosphere.

Other information about the dynamics of the system can be inferred from the PV distribution. This is best demonstrated by comparison between Figures 1a and 1b. The area where the tropopause is steeply sloped (Fig. 1a), east of the low, lies directly above a zone of steeply sloped isentropes in the lower atmosphere. The area where the 200-400 mb PV gradient (Fig. 1b) is largest (across the tropopause where it is nearly vertical within the cross-section) lies directly above the zone of largest temperature gradients below 500 mb. Thus, the zone of large PV gradient surrounding the upper low lies above the mid and lower tropospheric frontal zone. The magnitude of the PV gradient (intensity of the upper-level front) will be directly proportional to the intensity of the frontal zone in the lower troposphere.

Hoskins et al. (1985) describe the effect of an upper-air PV anomaly on the lower atmosphere. A PV anomaly developing over, or moving suddenly into an area, creates an atmosphere out of geostrophic balance. A pattern of ageostrophic motion will develop as the atmosphere strives to create a balanced state. A lower tropospheric cyclone and area of reduced static stability is "induced" by the upper-level feature. The authors state that lower atmospheric parcels approaching the anomaly in a relative sense will be lifted along isentropes as they are affected by the ageostrophic circulations. The PV anomaly acts as a "giant gentle vacuum cleaner", wherever it moves, lifting parcels ahead of it and causing descent of parcels in its wake. This concept is qualitatively indicated (Fig. 2) by the pattern of ageostrophic motion parallel to the cross-section.

In summary, the PV distribution is fundamental in diagnosing the middle and lower tropospheric baroclinicity, static stability, and areas of vertical motion. The PV distribution also depicts the location and relative intensity of the jet stream and the upper-level front.

The Operational Technique

PC-GRIDDS macros have been developed to calculate PV (Fig. 3) within various atmospheric layers (Appendix 1). The principal application has been to identify upper-level fronts and their intensity and movement. Ertel's PV is calculated, except that a layer average absolute vorticity is substituted for the absolute vorticity on an isentropic surface. Layer average wind and advection of the layer PV by that wind are also included in the diagrams. The intensity of the advection is directly a function of the strength of the wind, the magnitude of the wind normal to the PV field (and thus normal to the upper front), and the intensity of the upper front itself. In areas of large positive PV advection, intense warm advection will be occurring aloft and ageostrophic motion in the middle and lower troposphere will be significant (Hoskins et al. 1985 and Hirschberg and Fritsch 1991). Positive PV advection is correlated with synoptic-scale areas of ascent in the middle troposphere and negative PV advection with descent. The PV values are contoured every 0.5 PV units after Hoskins et al. (1985). One PV unit is equivalent to 10^{-6} m^2 s^{-1} K kg^{-1}.

The PV distribution (Fig. 3) shows an area of relatively high values of PV within the large-scale trough over the western United States. The polar jet lies within the zone of PV gradient surrounding the low and the polar front will be present in the middle and lower tropopause below this zone. Shortwaves within the polar jet are delineated by couplets of positive and negative PV advection. In this case, a strong shortwave is present in the base of the trough with a weaker shortwave located over the northern California coast. Dynamics producing synoptic-scale lift are strongest over the junction of the Nevada, Utah, and Arizona state borders where the area of positive PV advection is centered. There is also a complex pattern of shortwaves affecting south central Canada and the northern Mississippi Valley. A ridge is clearly indicated over the eastern Pacific Ocean.

PV is not conserved within these diagrams, which are constructed within deep isobaric layers. The values of PV increase or decrease as tropopause undulations descend or form in the layer, or weaken and decrease in vertical extent and intensity. The technique presented here does not identify tropopause folds (Bluestein 1986), although they would, and do occur along the upper front, or within the zone of large PV gradients. The PC-GRIDDS data that is distributed to the field has relatively poor resolution in the vertical since it is limited to mandatory levels. This limited vertical resolution may reduce the effectiveness of attempting to quantify the strength of tropopause folds and the magnitude of PV advection on isentropic surfaces. Rather, this analysis evaluates the forecast strength and movement of upper-level fronts, associated with synoptic-scale disturbances, and their position relative to lower atmospheric heat and moisture sources.

Case Examples

Examples are presented below to illustrate the relationship between upper-level frontal zones and shortwaves, identified with an analysis of PV, and areas of vertical motion in the troposphere. Diagrams of the distribution of PV illustrate the upper-level features. The 700 mb equivalent potential temperature (θ_e) and winds illustrate the middle tropospheric frontal zones and moisture sources. Accumulated rainfall and lightning data are used to define where significant weather was observed.

July 5-6, 1994

During 5-6 July 1994; an intense upper low dominated the weather over the western United States (Fig. 4a). The low moved across Oregon on 5 July (Fig. 4b) and to southeast Idaho by 1200 UTC 6 July (Fig. 4c). This system was responsible for an outbreak of severe weather across parts of the interior West and locally heavy rainfall. A dry cold front accompanying the system contributed to the explosive fire behavior on the South Canyon incident in Colorado during the afternoon of 6 July. A wetting rain was observed during the 24 hours ending 1200 UTC 6 July in a band stretching from northeast Oregon to east central Montana (Fig. 5). Lightning was widespread (Fig. 6), especially in Wyoming.

The PV gradients forecast with this low (Fig. 4), indicate an intense upper-level front, surrounding the low, weakening with time. In reality, the system moved more slowly than this forecast and maintained its intensity. PV advection is positive east of the low and negative west of the low. The PV distribution and advection pattern clearly describe the synoptic-scale pattern forecast by the NGM.

At 700 mb, a θ_e ridge was present over the Rocky Mountains (Fig. 7), indicative of warm and moist air. Some of the heavy rainfall in southwest Montana is undoubtedly orographic as the warm and moist air-mass, diagnosed by the 700 mb θ_e ridge, is pulled westward and into the Rocky Mountains by the cyclone. Rainfall and lightning accompanied the areas of PV advection as they moved eastward with the upper low. Advection of the 200-400 mb PV, by the layer average wind, summed for the 24 hour period ending 1200 UTC 6 July (Fig. 8), agrees well with the areas of lightning, rainfall, and severe weather.

July 25, 1994

A second example of the usefulness of PV diagnosis was an outbreak of evening lightning over Washington and Oregon. Figure 9 is a two-hour summary of detected lightning strikes ending at 0015 UTC 25 July, 1994. The 700 mb (Fig. 10), analysis from the NGM, includes a pronounced θ_e ridge the western United States, with an area of negative θ_e advection along the west coast. The 200-400 mb PV diagrams for 0000 and 0600 UTC 25 July (Fig. 11a and 11b) illustrate the PV anomaly, or upper-level shortwave, and the PV advection pattern moving northward over Oregon and Washington.

This upper-air disturbance was well-defined. For example, there was significant differential vorticity advection associated with the trough. Thunderstorms over Washington and Oregon continued well into the evening. Lightning activity over the Rockies and high plains, in the θ_e ridge axis, diminished rapidly after sunset. The 200-400 mb PV diagrams for this case indicate the fundamental difference between the two areas of convection. There was very little positive PV advection indicated over the Rockies, and thus very little upper air dynamics to provide lift on the synoptic- scale.

Summary

Potential vorticity is easily calculated operationally, within upper-tropospheric layers, using the PC-GRIDDS software. The forecast PV distribution describes the location and relative strength of synoptic-scale features aloft, including subtle shortwaves, which determine the patterns of synoptic-scale vertical motion in the middle and lower troposphere. These features are associated with the ageostrophic motions which are commonly estimated, in the operational setting, using a variety of techniques within the quasi-geostrophic framework. Hoskins et al. (1985) argue that rather than using traditional vorticity advection fields, the use of PV advection "avoids the dangers inherent in traditional vorticity arguments".

Acknowledgments

I would like to thank John Jannuzzi, Rusty Billingsley, and Western Region SSD for reviewing this paper.

References

Bluestein, H.B., 1986: Fronts and Jet Streaks: A Theoretical Perspective, *Mesoscale Meteorology and Forecasting*, Edited by Peter S. Ray, American Meteorological Society, pg 173.

Hirschberg, P.A. and J.M. Fritsch, 1991: Tropopause Undulations and the Development of Extratropical Cyclones. Part II: Diagnostic Analysis and Conceptual Model. *Mon. Wea. Rev.*, **119**, 496-517.

Holton, J.R., 1992: *An Introduction to Dynamic Meteorology*, Academic Press, New York, New York, 511 pp.

Hoskins, B.J., M.E. McIntyre and A.W. Robertson, 1985: On the Use and Significance of Isentropic Potential Vorticity Charts. *Quart. J. Roy. Meteor. Soc.*, **111**, 877-946.

Keyser, D., 1986: Atmospheric Fronts: An Observational Perspective, *Mesoscale Meteorology and Forecasting*, Edited by Peter S. Ray, American Meteorological Society, pg 216.

Meier, K.W., 1993: PCGRIDS Users's Manual, NWS Scientific Services Division, Western Region Headquarters, 26 pp.

Appendix 1. Sample PV Macro's

200-400 mb layer Potential Vorticity

```
loop
SLVL 300
slyr 400 200
SMLC 9.81 smlt vort wind lave stab c5-5 clr3
dneg dotp wind ngrd smlc 9.81 smlt vort wind lave stab c2-9 clr2&
wind SLVL 300 arow clr1&
txt3 POTENTIAL VORTICITY GRADIENTS (WHITE) = UPPER-LEVEL FRONTAL ZONES
AND THE JET CORE.
TXT4  POSITIVE ADVECTION (solid red) = SYNOPTIC SCALE LIFT DUE TO UPR FNT.
endl stop
```

Cross-Section of PV and vertical velocities

this macro needs to be expanded to accommodate other forecast times.

```
loop
xsct
c5-6 sneg smlt wvrt lvl0 sdvd sdif thta lv+1 thta lv-1 sdif pres lv+1 pres lv-1
vvel lt00 clr2 c1-3/
vvel gt00 clr5 dash c1-3/
xlbl nlbl pres clr3/
xlbb nlbl latt clrf/
xlbb nlbl datt long clrf/
txt3 Cross-section of Potential vorticity (purple) and vertical velocity
txt4  red for upward, blue (dashed) for downward. PVU's near 1-1.5 = tropopause.
plan
endl
```

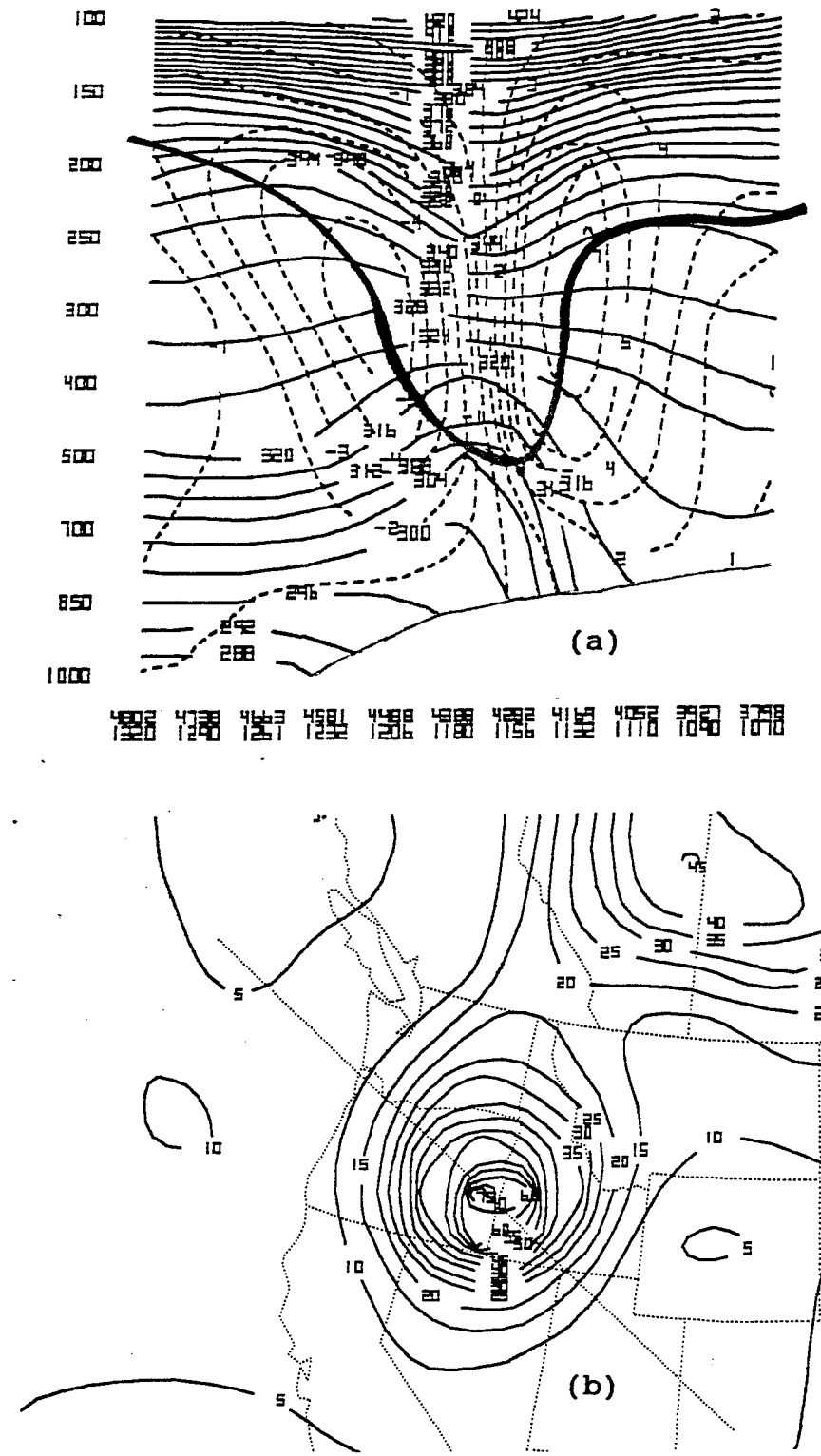

Figure 1. NGM initialized data at 0000 UTC 6 July 1994 for (a) a cross-section of θ (solid) every 4K, isotachs (dashed) every 10 knots of the wind component normal to the cross-section (positive values into the page) and the tropopause (heavy black line) located where the potential vorticity equals 1.5 PV units and (b) potential vorticity in the 200 to 400 mb layer every 0.5 PV units. The location of the cross-section of Fig. 1a and Fig. 2 is also indicated by the solid line through the upper low. Data below ground within the NGM has been removed from the cross-section.

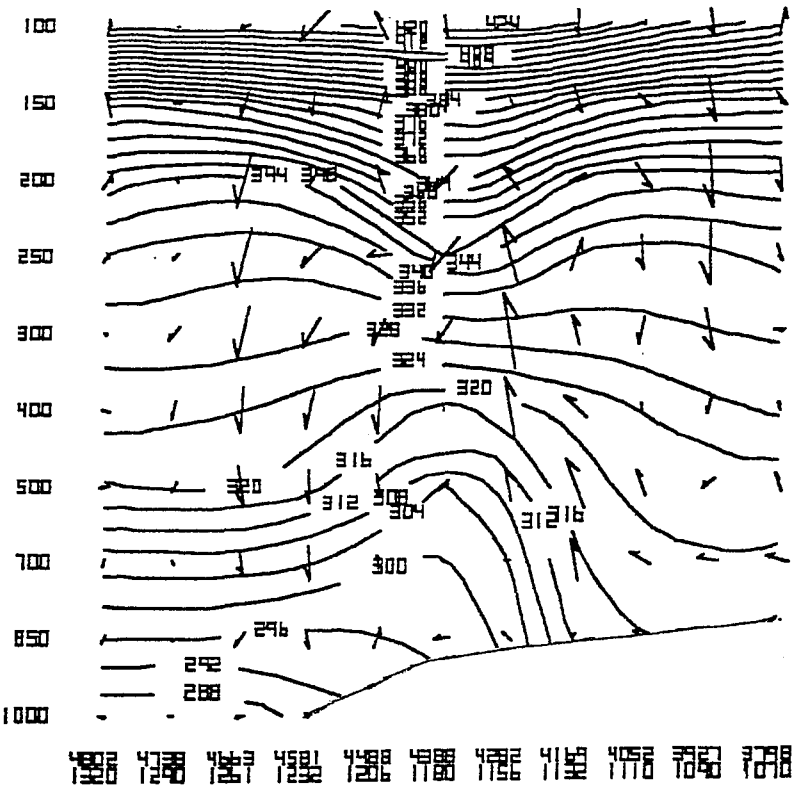

Figure 2. NGM initialized data at 0000 UTC 6 July 1994 along a cross-section of θ (solid) every 4K and ageostrophic wind vectors (arrows). Data below ground within the NGM has been removed.

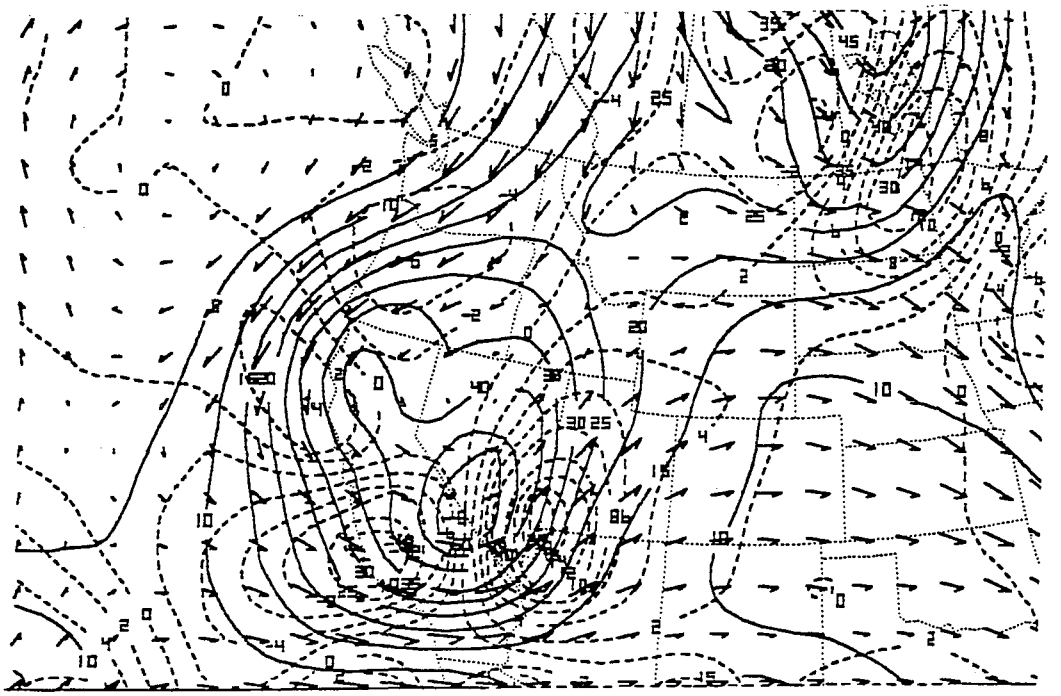

Figure 3. NGM initialized data at 1200 UTC 8 February 1995 for 200 to 400 mb layer potential vorticity (solid) every 0.5 potential vorticity units, advection of the potential vorticity by the layer averaged wind (dashed) every 2×10^{-9} IPV Units s^{-1} and 200 to 400 mb layer average wind (arrows).

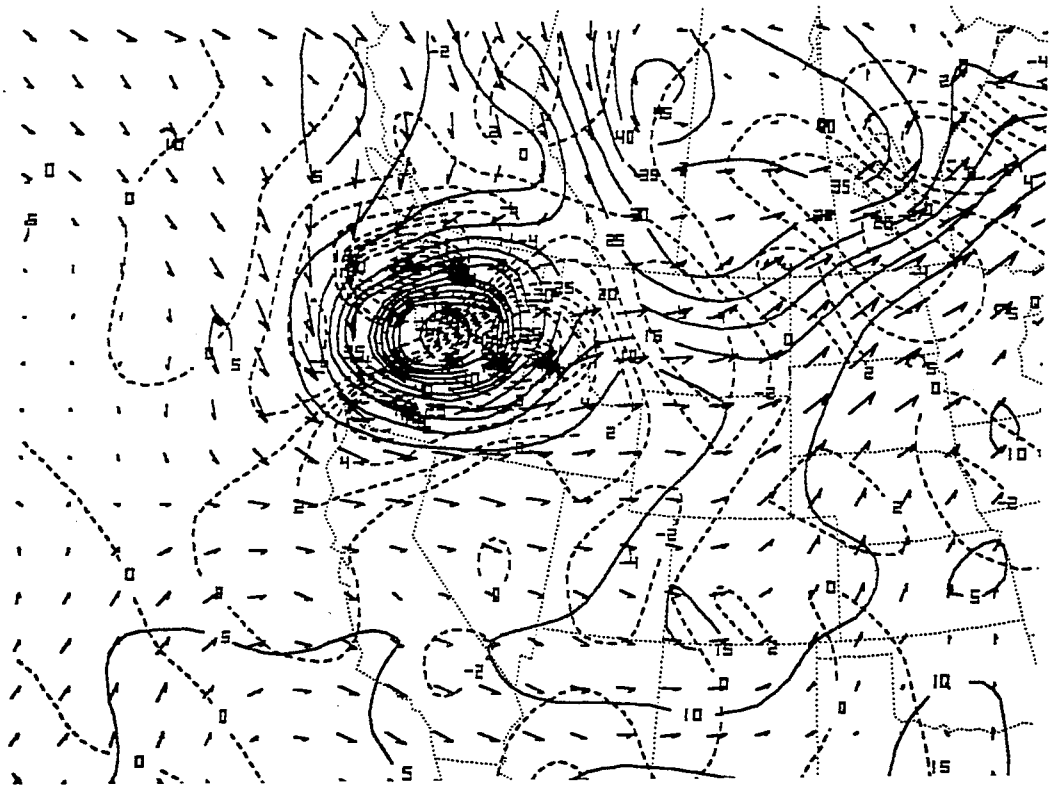

(a)

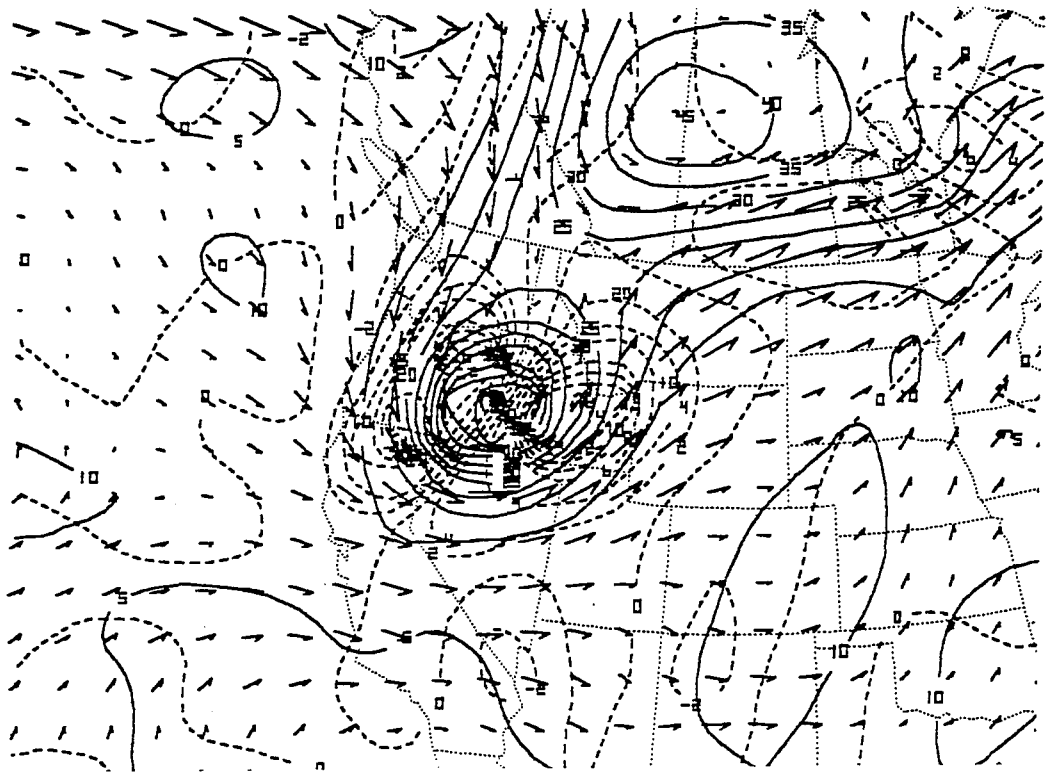

(b)

Figure 4. Same as in Fig. 3 except forecast data for (a) 1200 UTC 5 July, (b) 0000 UTC 6 July and (c) 1200 UTC 6 July 1994.

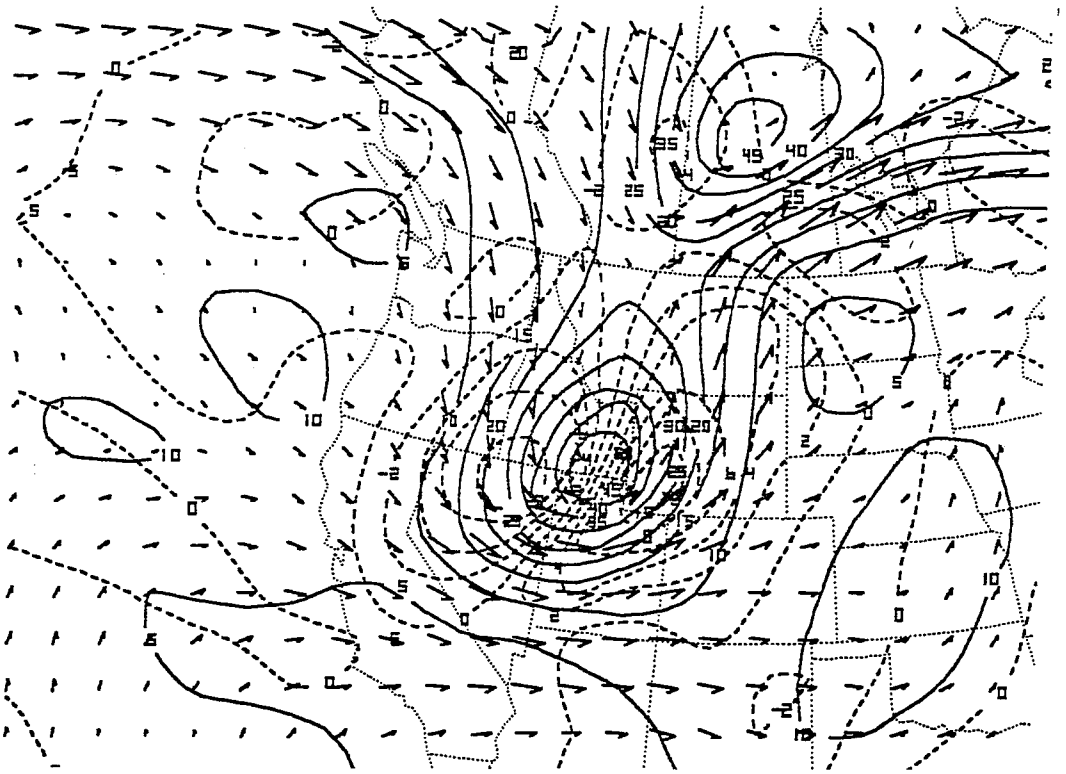

Figure 4 c

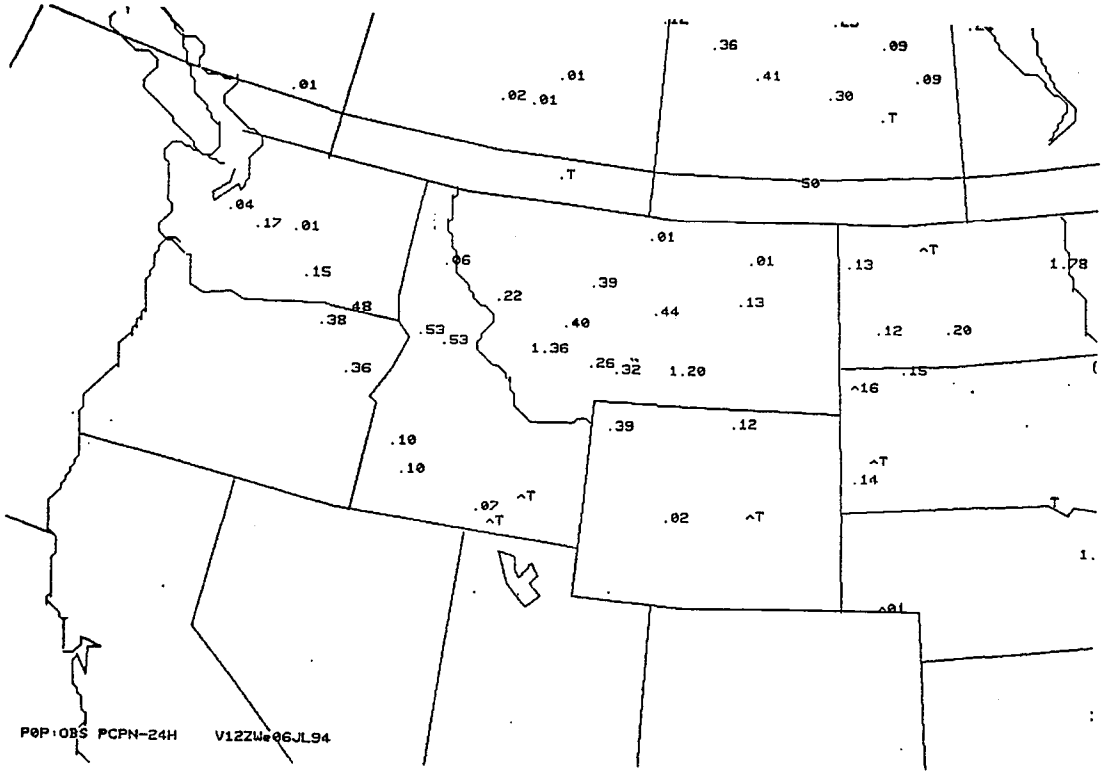

Figure 5. 24 hour accumulated precipitation valid 1200 UTC 6 July 1994.

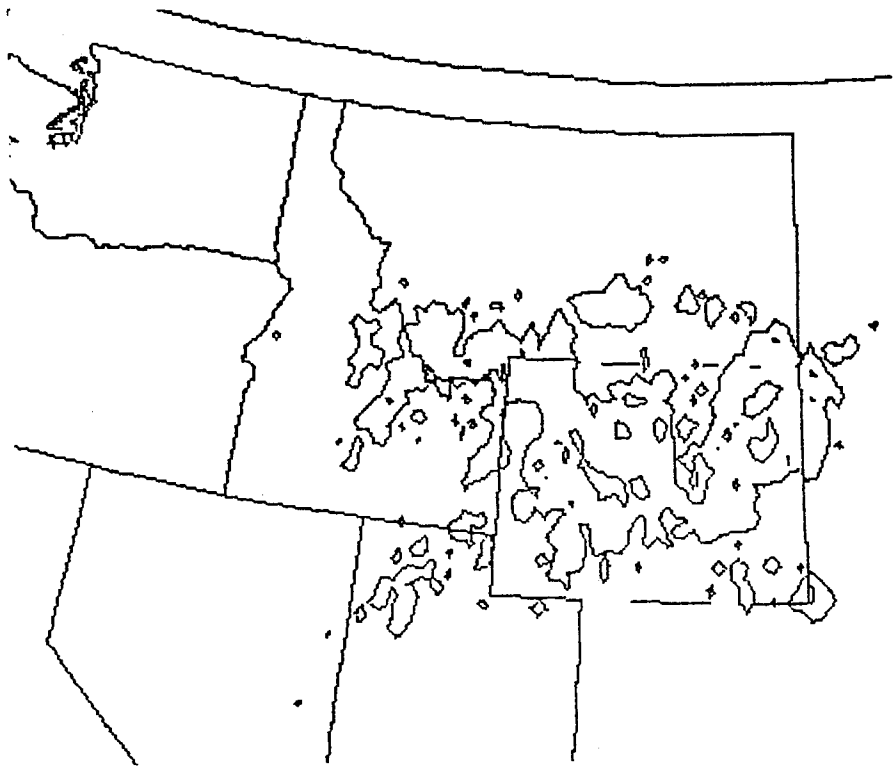

Figure 6. Lightning detected during the 24 hour period ending 1215 UTC 6 July 1994.

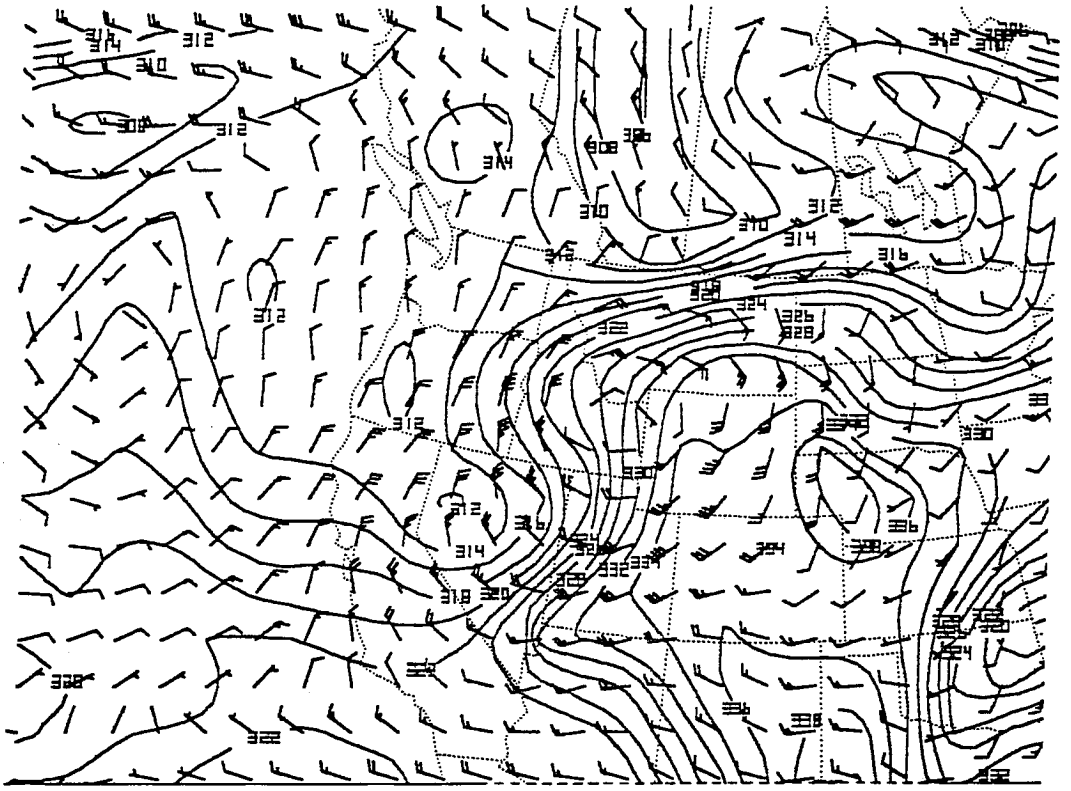

Figure 7. NGM forecast of 700 mb θ_e (solid) every 2K and wind (barbs) in knots valid 0600 UTC 6 July.

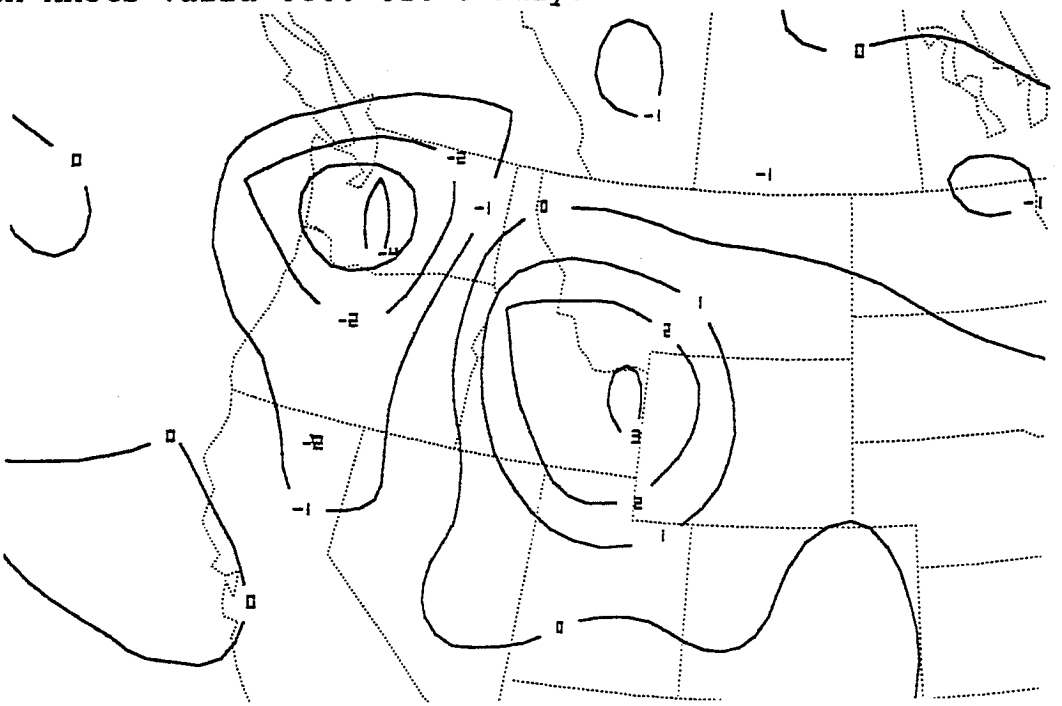

Figure 8. Accumulated advection of 200 to 400 mb potential vorticity by the layer average wind every 10^{-8} IPV Units s^{-1}.

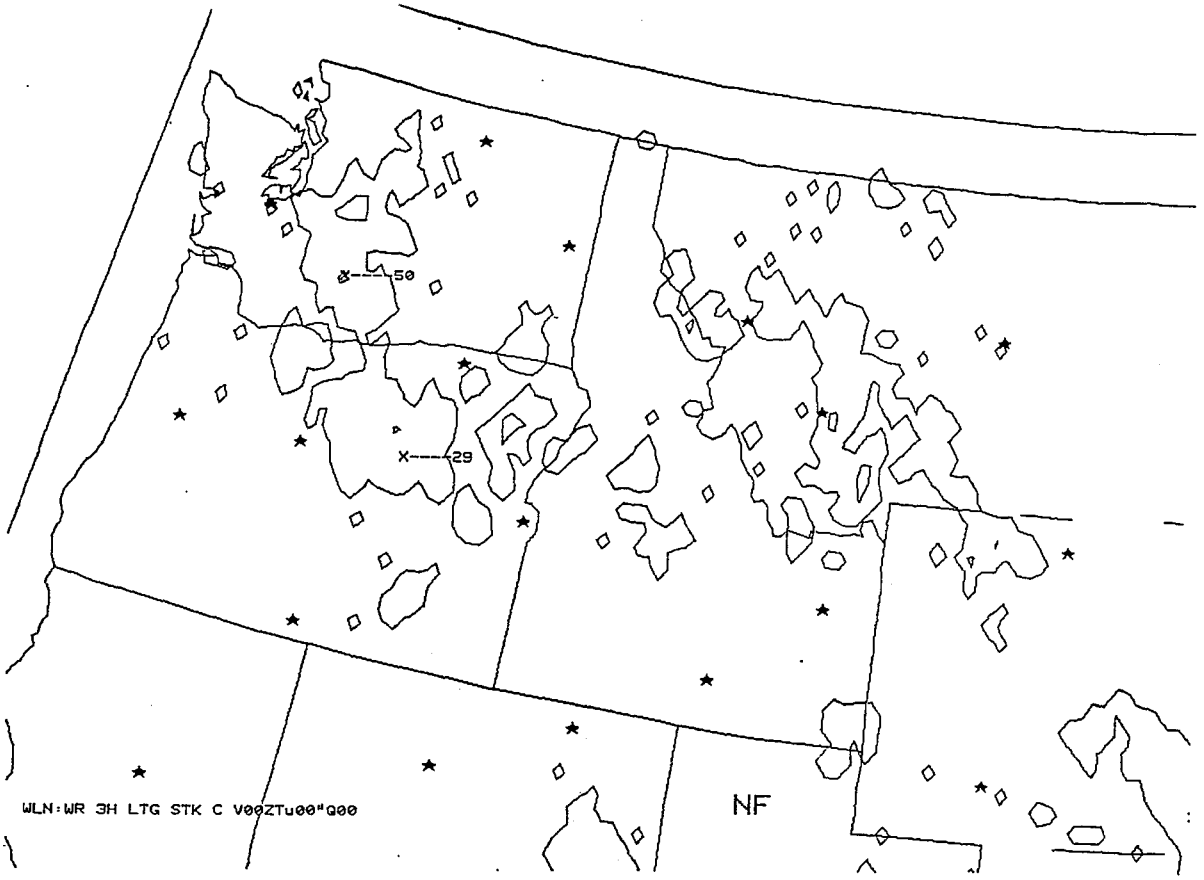

Figure 9. Lightning detected during a 2 hour period ending 0015 UTC 25 July 1994.

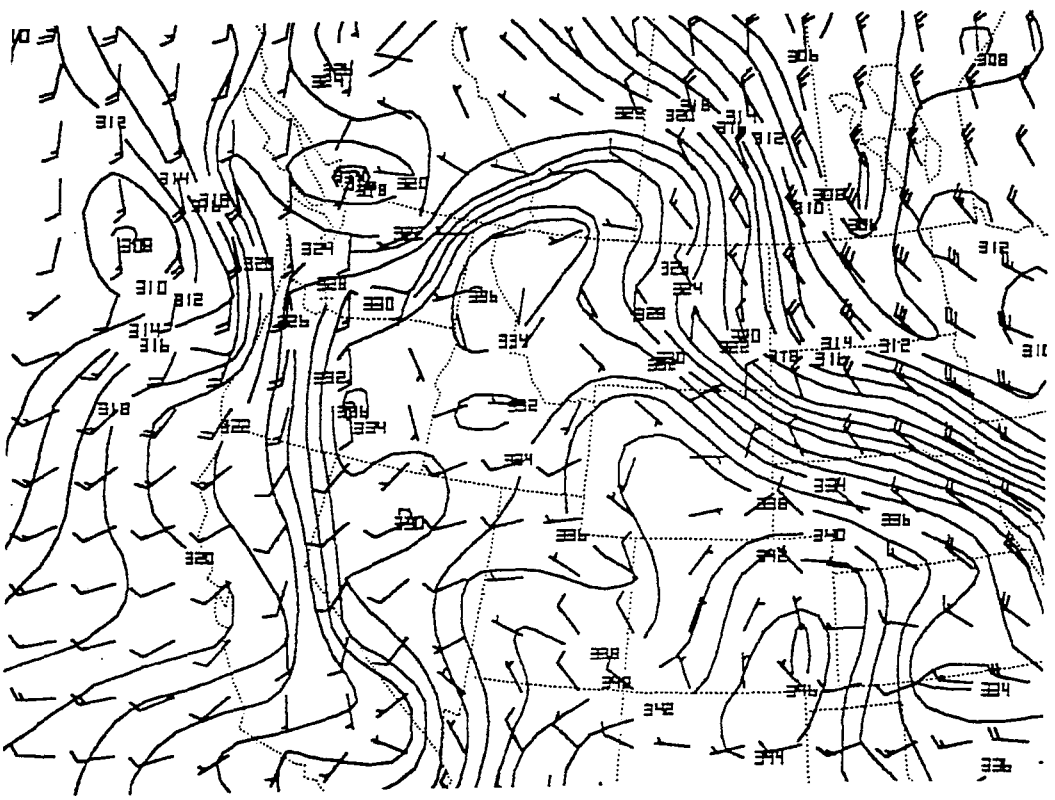

Figure 10. NGM forecast of 700 mb θ_e (solid) every 2K and wind (barbs) in knots valid 0000 UTC 25 July.

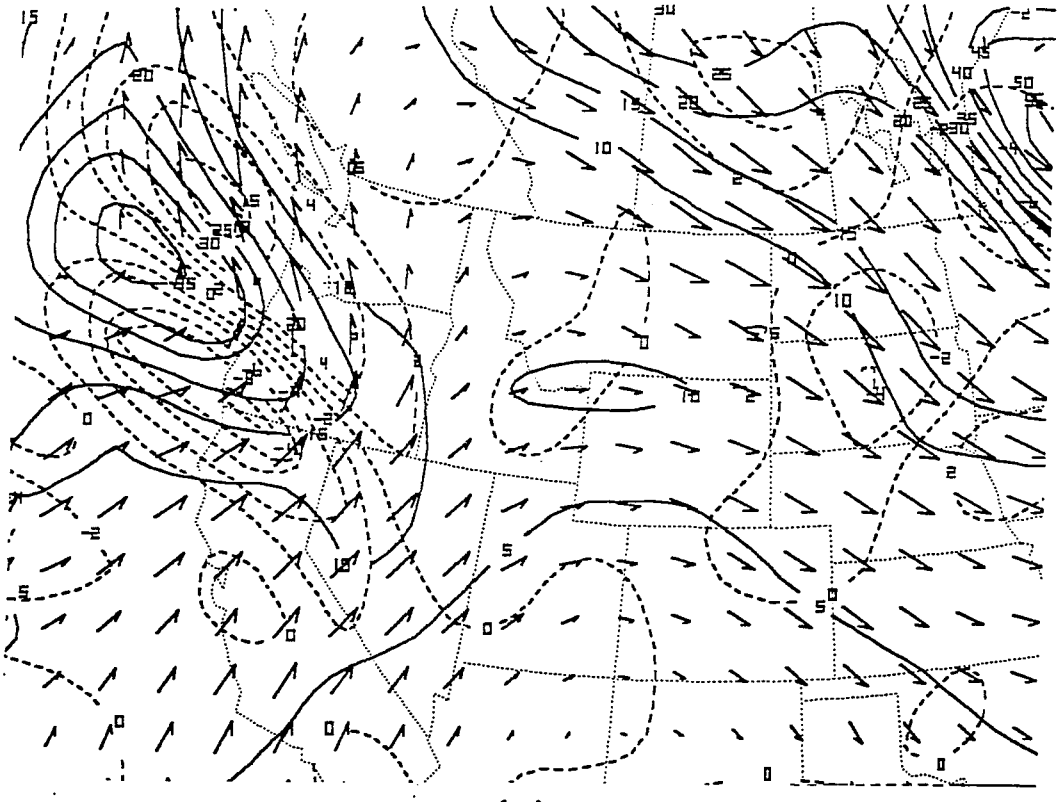

(a)

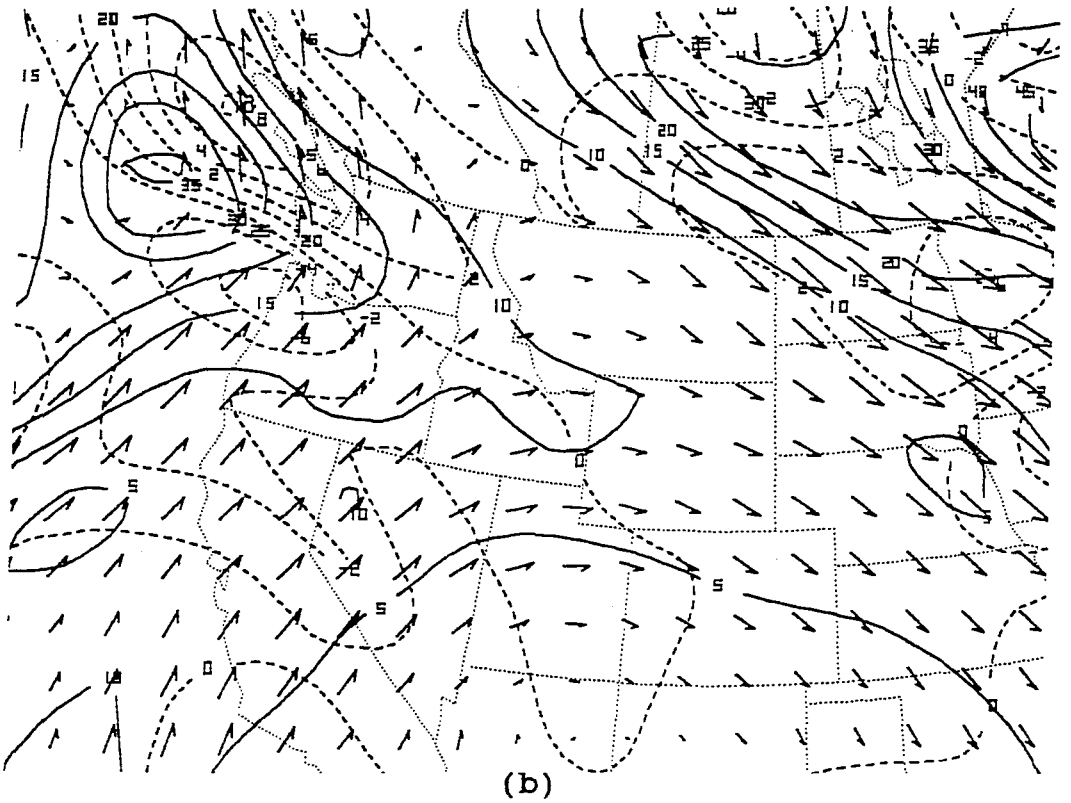

(b)

Figure 11. Same as in Fig. 3 except forecast data for (a) 0000 UTC 25 July, (b) 0600 UTC 25 July 1994.22